ministerie van verkeer en waterstaat

koninklijk nederlands meteorologisch instituut

An improved wind input source term for third generation ocean wave modelling

L. Yan

scientific reports WR-nr 87-8

wetenschappelijke rapporten WR-nr 87-8

de bilt, 1987

de bilt 1987 publicationnumber: Scientific reports = wetenschappelijke rapporten ; WR 87-8 (00)

p.o. box 201
3730 AE de bilt
wilhelminalaan 10
tel.+31 30 766911
telex 47096

Division of Oceanographic Research

U.D.C.: 551.466.33
551.556.8

ISSN: 0169-1651

An improved Wind Input Source Term for Third Generation Ocean Wave Modelling

L. Yan

Abstract

Measurements by Snyder et al (1981) in the Bight of Abaco have shown that the growth rate of wind generated surface gravity waves can be approximated by a relationship $\beta = \frac{dE}{Edt} = (0.25 \pm 0.05).\varepsilon. (\frac{U_5}{c} \cos\theta - 1)\ \omega$ for $1 < \frac{U_5}{c} < 3$, which, for a given U_5 , is valid for relatively low frequencies. A revised form of this expression, $\beta = 0.25\ \varepsilon\ (28 \frac{U^*}{c} \cos\theta - 1)\ \omega$ was proposed by Komen et al (1984) on the argument that friction velocity is a better scaling parameter considering the dependence of the drag coefficient C_d on wind speed. A different expression for β was given by Plant (1982). It has the form $\beta = (0.04 \pm 0.02) \frac{\omega U^{*2}}{c^2} \cos\theta$, which is in agreement with a variety of both tank and field measurements in the high frequency range with a fixed U*. In this note, a new expression is presented, combining Komen's relation with Plant's relation. It has the form $\beta = \omega\ (0.04 \frac{U^{*2}}{c^2} \cos\theta + 0.00544 \frac{U^*}{c} \cos\theta + 0.000055\ \cos\theta - 0.000311)$. The effect of incorporating this formula in the WAM model is compared with the standard WAM model. It is found that the shifting of the spectral peak towards the low frequencies is somewhat slower and that the height of the peak has decreased somewhat. However, there is no strong influence on the energy gain by waves.

Introduction

The physical mechanism of the generation of surface gravity waves by wind has long been the focus of interest, especially after Miles' work on shear flow

instability (Miles, 1957). In his theory, the imaginary part of the wave induced pressure perturbation, with the same phase as the slope, does work on the wave and hence causes it to grow exponentially. Since then, many efforts have been made to verify this theory and to make it applicable. A recent experiment conducted in the Bight of Abaco (Snyder et al, 1981) measured growth rates in agreement with the Miles' theory and produced an approximation of these growth rates:

$$\gamma = (0.25 \pm 0.05).\varepsilon.\ (\frac{U_5}{c}\cos\theta - 1) \qquad (1)$$

where γ is the growth rate parameter β scaled by angular frequency ω; U_5 is the wind speed at the height of 5 m; c is the phase velocity; ε is the ratio of air density to sea water density ($\varepsilon \approx 1.25 \times 10^{-3}$); and θ is the propagation direction relative to the direction of wind. The validity of this formula is roughly $1 < \frac{U_5}{c} < 3$, since the data sets used are in that range. For a fixed wind speed U_5, the corresponding frequency range $g/2\pi U_5 < f < 3g/2\pi U_5$ contains relatively low frequencies. Thus it can not provide information on growth rate behavior reliably in the high frequency range. Yet this high frequency range is important: considerable energy input from atmosphere to surface waves occurs in this range. Considering the importance of scaling wave growth parameters with friction velocity rather than a wind speed at a fixed height (Janssen, Komen and de Voogt, 1985), Komen et al (1984) revised the above expression using friction velocity U*. They obtained

$$\gamma = 0.0003\ (28\ \frac{U^*}{c}\cos\theta - 1) \qquad (2)$$

which at present is incorporated in the so-called WAM model (Hasselmann et al, 1987). In 1982, after investigating a wide variety of measurements for both wave-tank and ocean fields by Shemdin and Hsu (1967), Larson and Wright (1975), Plant and Wright (1977), Wu (1977, 1979), Stewart ant Teague (1980), Plant (1982) proposed another growth rate relation:

$$\gamma = (0.04 \pm 0.02)\ \frac{U^{*2}}{c^2}\ \cos\theta \qquad (3)$$

over a wide frequency range from $g/2\pi U_{10}$ to 20 Hz. Although this relation is similar to those obtained in a number of theoretical studies and is quite

consistent with the experimental data over a rather high frequency range, it is not so good in the low frequency range, say around $f = g/2\pi U_{10}$.

In order to overcome the shortcomings of the two relations mentioned above, a new expression (we call it "fit" in the following) is proposed in this note, which, combining the two relations together, roughly reproduces eq. (2) in the low frequency range and eq. (3) at high frequencies.
The fit is used in the WAM model as a wind input source term to investigate its effect on wave growth. It has a tendency to reduce the spectral peak and to slow down its shift toward lower frequencies. However, there is no evident effect on the total energy gained by the waves. All other features of wave growth develop as in the standard WAM model. This is because the frequency range involved is rather low and there the difference between the fit and eq. (2) is small.
The plan of this note is as follows: in section 1, we will give the derivation of the fit; in section 2, the information on how the fit was incorporated in the WAM model is described; in section 3, model results are discussed and finally, in section 4, general conclusion will be drawn from the above.

Section 1 - Derivation of the fit

For clarity, Komen's relation and Plant's relation are rewritten as follows:

$$\gamma_k = A\,(x\cos\theta - B) \qquad (2')$$

$$\gamma_p = C\,x^2\cos\theta \qquad (3')$$

where $x = U^*/c$ and A, B, C are constants with the values 0.0084, 0.036 and 0.04 respectively.
As mentioned in the Introduction, eq. (2') gives a fairly good growth rate over the low x range, and on the contrary, eq. (3') behaves better over the high x range. This gives two constraints for the fit we are going to invoke. We take the form of the fit as

$$\gamma_f = Dx^2\cos\theta + Ex\cos\theta + F\cos\theta + H \qquad (4)$$

where D, E, F are constants to be determined.

According to the constraints, the fit for one dimension should satisfy the two conditions below:

$$\gamma_f \approx \gamma_k \qquad \text{for x near B} \tag{5}$$

and

$$\lim_{x\to\infty} \gamma_f = \gamma_p \tag{6}$$

Comparing (3') with (4'), we find D = C.

Expanding x^2 as $x_0^2 + 2x_0 (x-x_0)$ in eq. (4) (x_0 in the vicinity of B), we get three relations:

$$\begin{aligned} A &= 2x_0D+E \\ F &= x_0^2D \\ H &= -Ax_0 \end{aligned} \tag{7}$$

We select $x_0 = 0.037$, so as to obtain good agreement at U*/c values observed in the Bight of Abaco. Then we have

$$\begin{aligned} D &= C = 0.04 \\ E &= A - 2x_0D = 0.00544 \\ F &= x_0^2D = 0.000055 \\ H &= -Ax_0 = -0.000311 \end{aligned} \tag{8}$$

Fig. 1 shows the curves for γ_k, γ_f and γ_p, from which we can see that for a given U* = 0.85.

$$\begin{aligned} &\gamma_f < \gamma_k \text{ for } f < 0.0986 \\ &\gamma_f \approx \gamma_k \text{ for } f = 0.0986 \\ &\gamma_f > \gamma_k \text{ for } f > 0.0986 \end{aligned} \tag{9}$$

Since Fig. 1 is drawn on x ($= \frac{U^*}{c}$) coordinate, the x value corresponding to f = 0.0986 is 0.054.

One should note that in the transition range of medium frequency γ_f is larger than both γ_k and γ_p. This comes about because we believe that the data points at high and low frequencies lie on one smooth curve.

Section 2 - Running WAM with the fit for Case II of SWAMP

To study its effect on wave growth we introduce our fit eq. (4) into the WAM model for the standard situation of Case II of the SWAMP study and compare its results with those obtained with Komen's relation (2) for the same case.
The test case (Case II) is briefly as follows: a stationary homogeneous wind field with friction velocity $U^* = 0.85$ and its direction $\theta^* = 0°$ (clockwise from the north) blows orthogonally offshore over a deep water area which covers 20 latitudes and 20 longitudes.
The initial spectrum is mean JONSWAP spectrum (Jonswap, 1973), and the spectrum at the coastlines remains zero for $t > 0$. The test period is 45 hours. The spectrum output points selected and geometry considered are indicated in fig. 2.
The WAM model is a highly sophisticated third generation wave forecasting model, in which the source function and the propagation term in the energy balance equation are integrated on two different time step levels with different methods (implicit integration for the source function and first order upwind difference scheme for the propagation term). Usually, the propagation time step is a multiple of the source function time step. For this special test case we take both the source function time step and the propagation time step identically as 20 min. For other details about the WAM model we refer to Hasselmann (1987).

Section 3 - Results and discussion

For the convenience of comparison, we attach to the parameters relevant to γ_f a subscript f, and correspondingly, the parameters relevant to γ_k a subscript k. We also give a name f_t to 0.0986 where $\gamma_f \approx \gamma_k$.
Looking into the resulting spectrum, we find that with γ_f WAM also can demonstrate all the well-known features of the growth of the spectrum, such as the overshoot effect, the shift of the spectral peak to lower frequencies, sharp peak, steep forward face and smooth backward slope, etc. However, when one looks at details of the spectral shape, there are some differences, which also have some effect on the growth curves.

At an early growth stage, when the dominant part of the spectrum falls beyond f_t or just over it, $F_f(f) > F_k(f)$ is true for all the spectral densities (see fig. 3). This can be entirely attributed to γ_f being larger than γ_k over the range $f > f_t$.

As it is developing, the main body of the spectrum goes gradually into the frequency range lower than f_t. Then, the migration speed of the spectral peak of F_f starts to slow down relative to that of F_k. Subsequently, the difference between the two spectra increases with time. This can be seen clearly in fig. 4 and fig. 5, which indicate the spectra for the same fetch at different durations, 21 h. and 45 h., respectively. Apparently, the spectra in fig. 4 are much closer to each other than those in fig. 5.

This phenomenon is readily explained if we recall one of the features of the nonlinear transfer. According to Hasselmann et al (Part I, 1985), the strongest interaction takes place around the spectral peak and this leads to a sharp low frequency positive lobe and an intermediate frequency negative lobe in the nonlinear transfer rate. For a sharply peaked spectrum of the JONSWAP form, the low-frequency positive lobe lies slightly to the left of the peak on the forward face of the spectrum and tends to grow the peak and move the spectrum towards the lower frequency range. The position and magnitude of the low-frequency positive lobe has a strong dependence on the shape of the spectrum, especially on the shape in the vicinity of the spectral peak. The reverse is also true. In this way, nonlinear transfer is an important element in the evolution of the wind wave spectrum.

When the spectrum has energy on either side of f_t, the growth rate of the form γ_f causes lower values for $f < f_t$, and higher values for $f > f_t$ for the spectrum than γ_k. Practically, this means that the peak of $F_f(f)$ is simply shifted a little bit to higher frequency as compared with that of $F_k(f)$. And also the shapes of the two spectra are different. These slight differences in the spectral peak locations and shapes (especially in the peak locations in our case, while shapes are rather similar) give rise to relative large variation of the spectral density around the peak, especially on the forward faces, and therefore are enhanced by the feature of nonlinear transfer mentioned above.

In the next time step, the different growth rate once more add their effect larger than the previous time step, because of enlarged disparity between the spectra, on the spectra. Then again, the nonlinear transfer acts, and so on. In this way, at the end we get the developed spectra of fig. 5, the difference being larger than that in fig. 4 which represents the spectra in an earlier growth stage.

Additionally, dissipation process also contributes to the phenomenon being discussed. The dissipation source term used in the WAM model has the form

$$S_{ds} \sim (E\bar{\omega}^4/g^2)^2 . \omega^2/\bar{\omega} \; . \; F$$

where E is the total energy and $\bar{\omega}$ is the mean angular frequency. The combined parameter $\alpha = E\bar{\omega}^4/g^2$ is the steepness of the waves, representing the state of development. The high power to which $\bar{\omega}$ is raised makes the source term S_{ds} very sensitive to the precise value of the mean frequency and therefore to the spectral shape.

At an early growth stage, the larger values of both $\bar{f}_f$ and E_f (to be discussed later) lead to a larger S_{dsf} term, retarding the development of $F_f(f)$. At a later developed stage, although $E_k > E_f$, we still have a S_{dsf} term larger than S_{dsk}, because of larger $\bar{f}_f$. That indicates that the dissipation source term also has influence on the slower shift of the spectrum $F_f(f)$, its reduced peak and energy.

As to the angular distribution, we find that γ_f is quite consistent with γ_k. The small discrepency between the two spectral at 30° and 60° is caused mainly by the effect of the nonlinear transfer coupling with different growth rates.

On the basis of the above analysis, it is not difficult to interpret differences in the fetch and duration limited growth curves for energy E, given by fig. 6 and fig. 7. For early growth stages, or at short fetches E_f has higher values than E_k. There are two reasons for this. First, at this stage, the two spectra are relatively closer to each other and the difference between the values of the spectral densities on the forward face is not so large, compared with more developed case. Second, because of a logarithmic scale of frequency adopted, the frequency steps over which a forward spectral face stands are much smaller than the steps for the backward spectral slope. So, the reduced energy caused by the smaller density values on the forward face of $F_f(f)$ is more than offset by the larger energy gain caused by the larger values of $F_f(f)$ over the frequencies above the peak frequency f_{pf}. For the fully developed case, we should say that large gap on the forward spectral faces of the two spectra contributes more than the gap on the backward slopes to the difference between E_f and E_k, causing $E_f < E_k$. Nevertheless, such a difference, $\max(|E_k - E_f|) \approx 0.23$, won't be regarded crucial in practical use.

Fig. 8 and fig. 9 give growth curves for the mean frequency $\bar{f}$ where $\bar{f}_f$ is always slightly higher than $\bar{f}_k$. Obviously, this can also be qualitatively explained by the above analysis of the slower shift of f_{pf}.

Section 4 - Conclusion

We combined Komen's relation (2), which is the revised form of Snyder et al (1981) and has a low validity range for U*/c, with Plant's relation (3), which is supported by many experiments for rather high U*/c range, into a single formula. To this end, a fit was explored with the form of (4). When used in the WAM model, in comparison with Komen's relation (2), γ_f slows down the migration of the spectrum towards low frequency range and tends to reduce the peak of the spectrum, coupling with the nonlinear and dissipation effect. Especially at high frequency, γ_f is much larger than γ_k. Yet, the effect on the gain of wave energy in the case considered is relatively small. And this is also true for the other well-known features of the wave growth in the wave evolution simulating model - WAM.

Acknowledgement: many thanks for the help given by Dr. G. Komen in my work and study at KNMI.

Figure captions

Fig. 1 Growth rate curves for $\theta = 0°$ (a) and $\theta = 30°$ (b). θ is the angle between wind and propagation directions. Arrows indicate the X points where $\gamma_f \approx \gamma_k$.

Fig.2 Geometry and points selected. Figures denote the fetches in km.

Fig. 3 Spectra $F_k(f)$ and $F_f(f)$ for the fetch 2200 km and duration 6 h, at propagation directions 0°, 30°, 60°, respectively. θ^* denotes the wind direction.

Fig. 4 and 5. The same as fig. 3 except for the duration being 21 h and 45 h.

Fig. 6 and 7. Fetch and duration limited growth curves of the energe E_k and E_f.

Fig. 8 and 9. Fetch and duration limited growth curves of the mean frequency $\bar{f}_k$ and $\bar{f}_f$.

References

G.J. Komen, S. Hasselmann and K. Hasselmann, 1984. On the existence of a fully developed wind-sea spectrum. J. Physical Oceanography 14 , 1271-1285.

S. Hasselmann and K. Hasselmann, 1985. Computation and parameterizations of the nonlinear energy transfer in a gravity-wave spectrum (Part I). J. Physical Oceanography 15, 1369 - 1377.

S. Hasselmann, K. Hasselmann, P.A.E.M. Janssen, G.J. Komen, L. Bertotti, A. Guillaume, V.C. Cardone, J.A. Greenwood, M. Reistad, J.A. Ewing, 1987. The WAM model - a third generation ocean wave prediction model (in preparation).

Miles J.W., 1957. On the generation of surface waves by shear flows, Part I. J. Fluid Mech., 3, 185 - 204.

Miles J.W. 1959. On the generation of surface waves by shear flows, Part II. J. Fluid Mech., 6, 568-582.

P.A.E.M. Janssen, G.J. Komen and W.J.P. de Voogt 1985. Friction velocity scaling in wind wave generation (in preparation)

Snyder R.L., F.W. Dobson, J.A. Elliott and R.B. Long 1981. Array measurements of atmospheric pressure fluctuation above surface gravity waves. J. Fluid Mech., 102, 1 - 59.

The SWAMP Group: J.H. Allender, T.P. Barnett, L. Bertotti, J. Bruinsma, V.J. Cardone, L. Cavaleri, J. Ephraums, B. Golding, A. Greenwood, J. Guddal, H. Günther, K. Hasselmann, S. Hasselmann, P. Joseph, S. Kawai, G.J. Komen, L. Lawson, H. Linné, R.B. Long, M. Lybanon, E. Maeland, W. Rosenthal, Y. Toba, T. Uji and W.J.P. de Voogt 1984. Sea Wave Modelling Project (SWAMP) Plenum Press

Plant W.J. 1982. A relationship between wind stress and wave slope. J. Geophysical Research, 87, No. C3,1961-1967

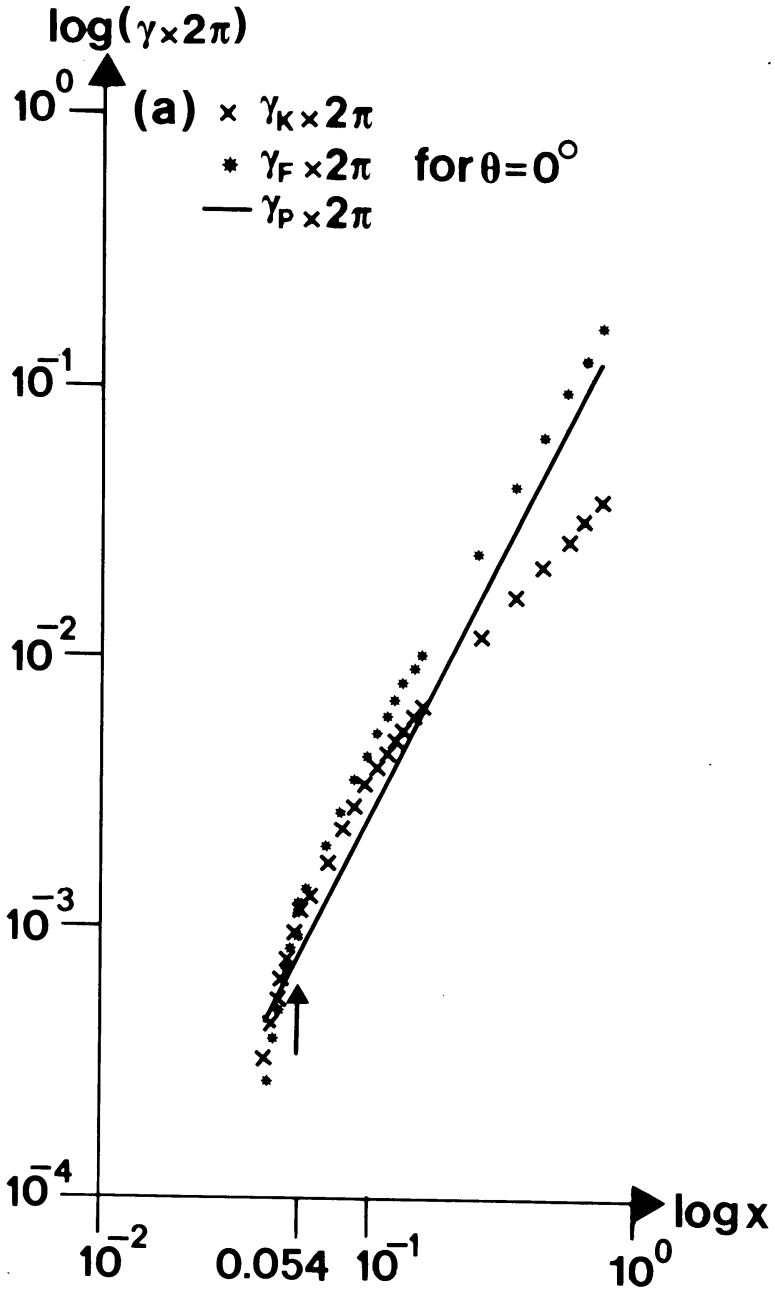
log(γ×2π)
10^0
(a) × γK×2π
* γF×2π for θ=0°
— γP×2π
10^-1
10^-2
10^-3
10^-4
log x
10^-2
0.054
10^-1
10^0
Fig 1a

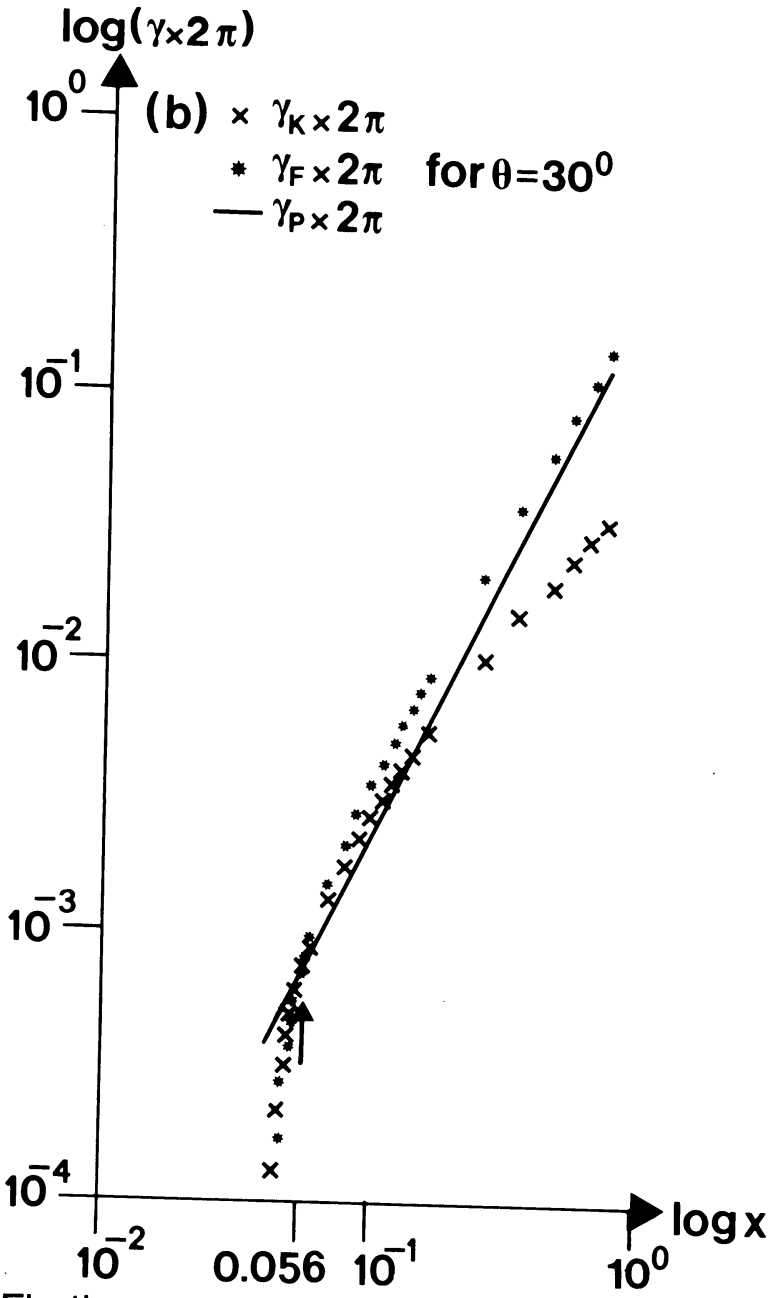
log(γ×2π)
10^0
(b) × γK×2π
* γF×2π for θ=30^0
— γP×2π
10^-1
10^-2
10^-3
10^-4
10^-2
0.056
10^-1
10^0
log x
Fig 1b

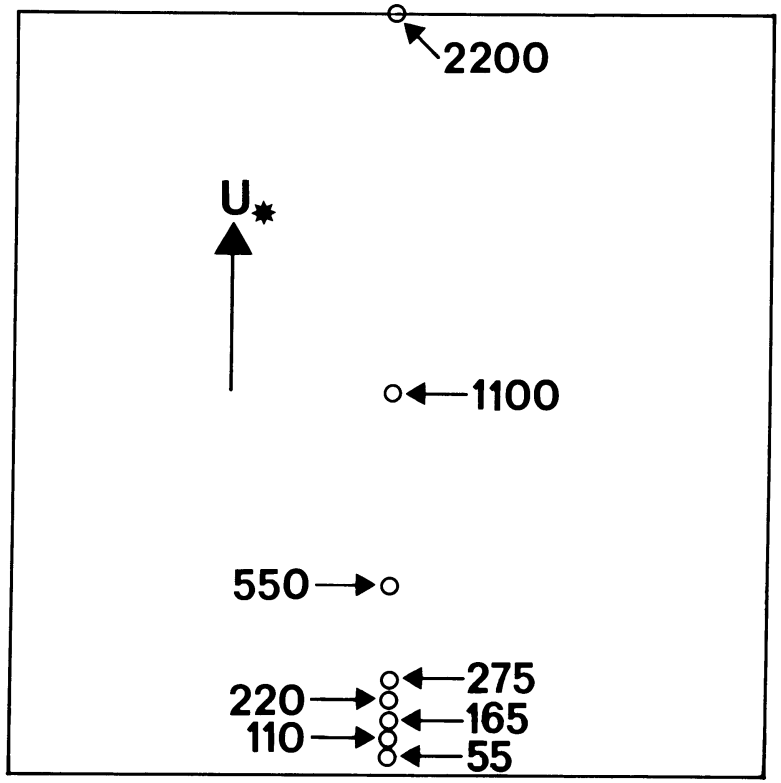

Fig 2

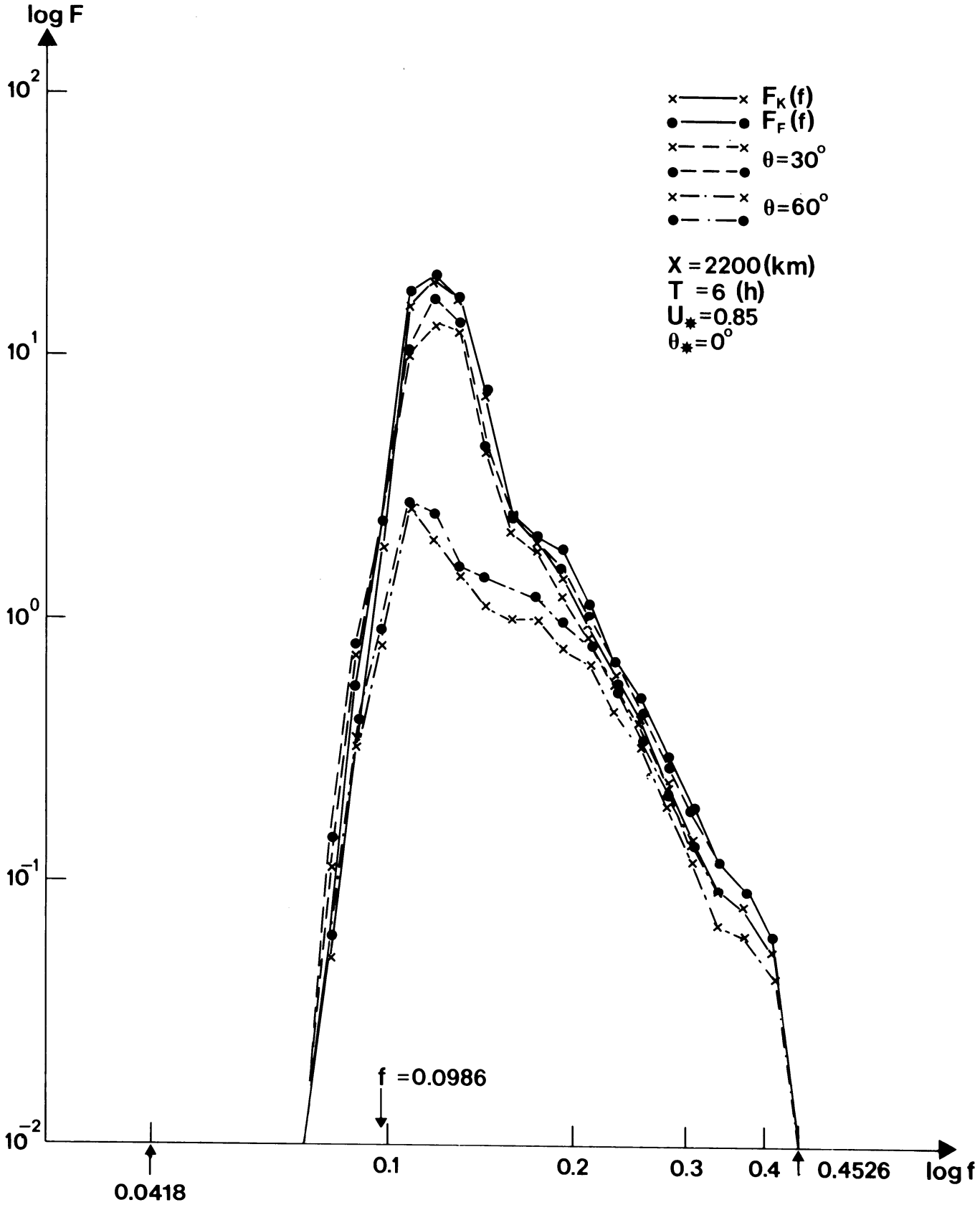
log F
10^2
10^1
10^0
10^{-1}
10^{-2}
$F_K(f)$
$F_F(f)$
θ=30°
θ=60°
X = 2200(km)
T = 6 (h)
U_*=0.85
θ_*=0°
f =0.0986
0.0418
0.1
0.2
0.3
0.4
0.4526
log f

Fig 3

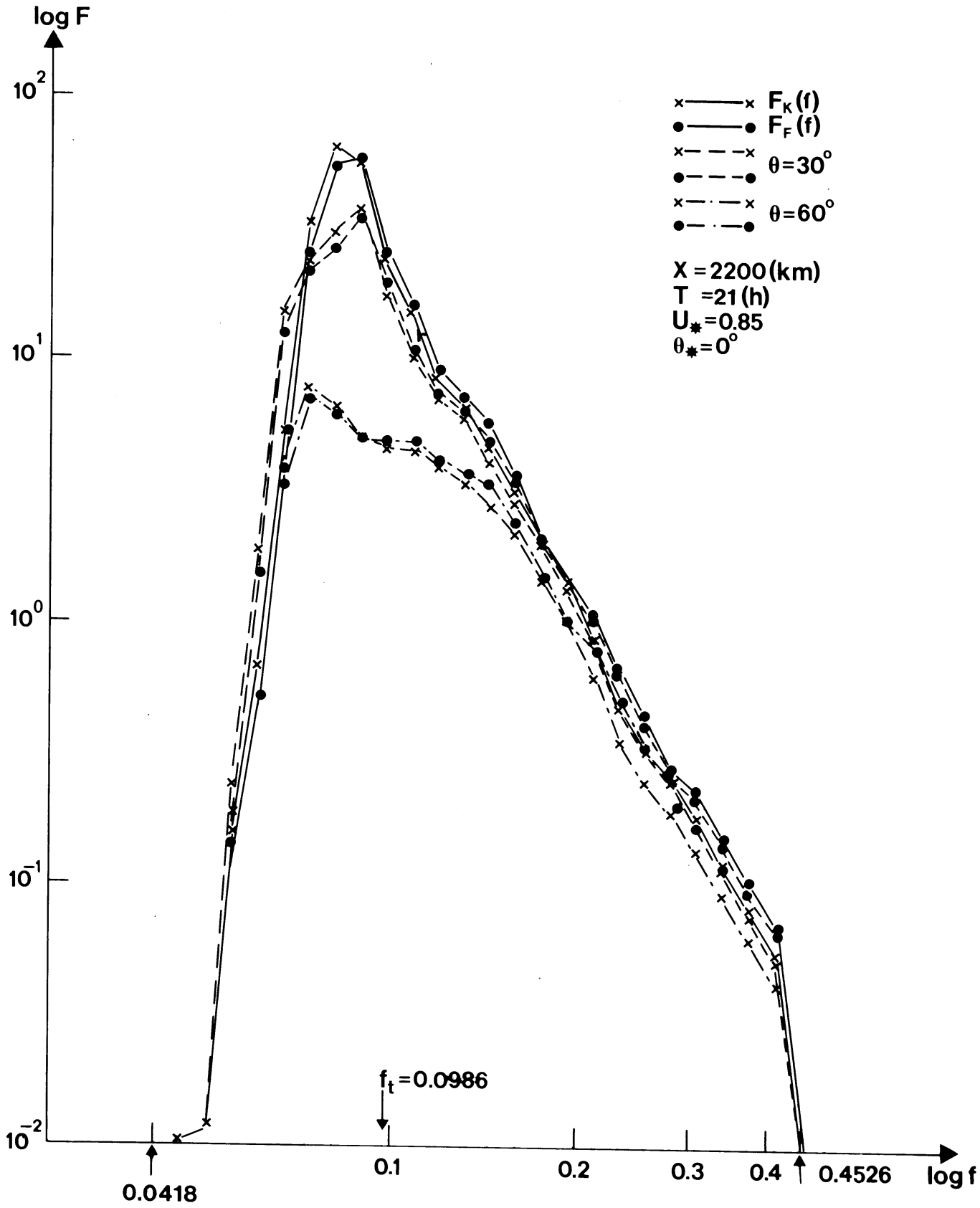
log F
10^2
10^1
10^0
10^{-1}
10^{-2}
$F_K(f)$
$F_F(f)$
θ=30°
θ=60°
X = 2200 (km)
T = 21 (h)
U_*=0.85
θ_*=0°
f_t=0.0986
0.0418
0.1
0.2
0.3
0.4
0.4526
log f

Fig 4

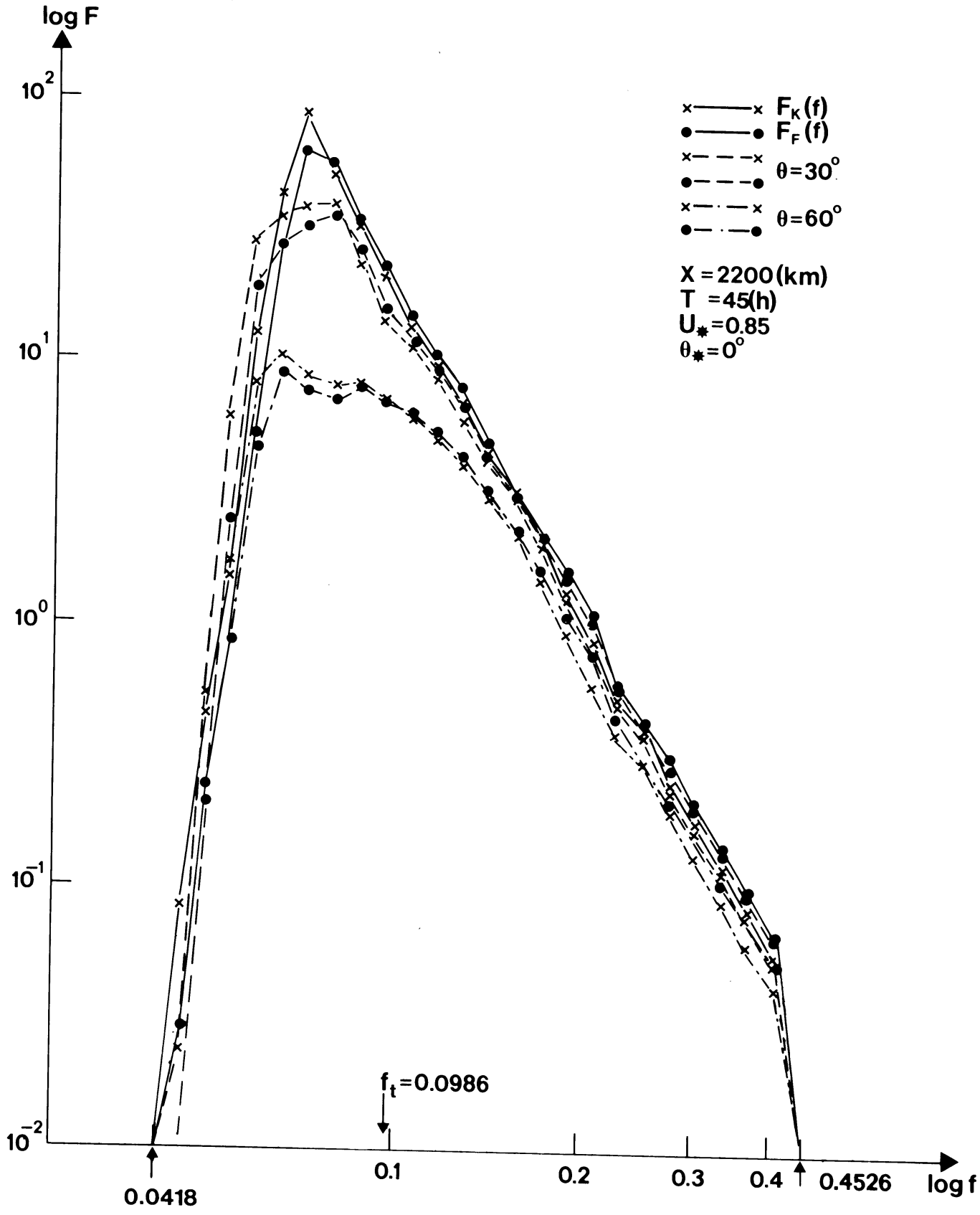
log F
10^2
10^1
10^0
10^{-1}
10^{-2}
$F_K(f)$
$F_F(f)$
θ=30°
θ=60°
X = 2200 (km)
T = 45(h)
$U_* = 0.85$
$\theta_* = 0°$
$f_t = 0.0986$
0.0418
0.1
0.2
0.3
0.4
0.4526
log f

Fig 5

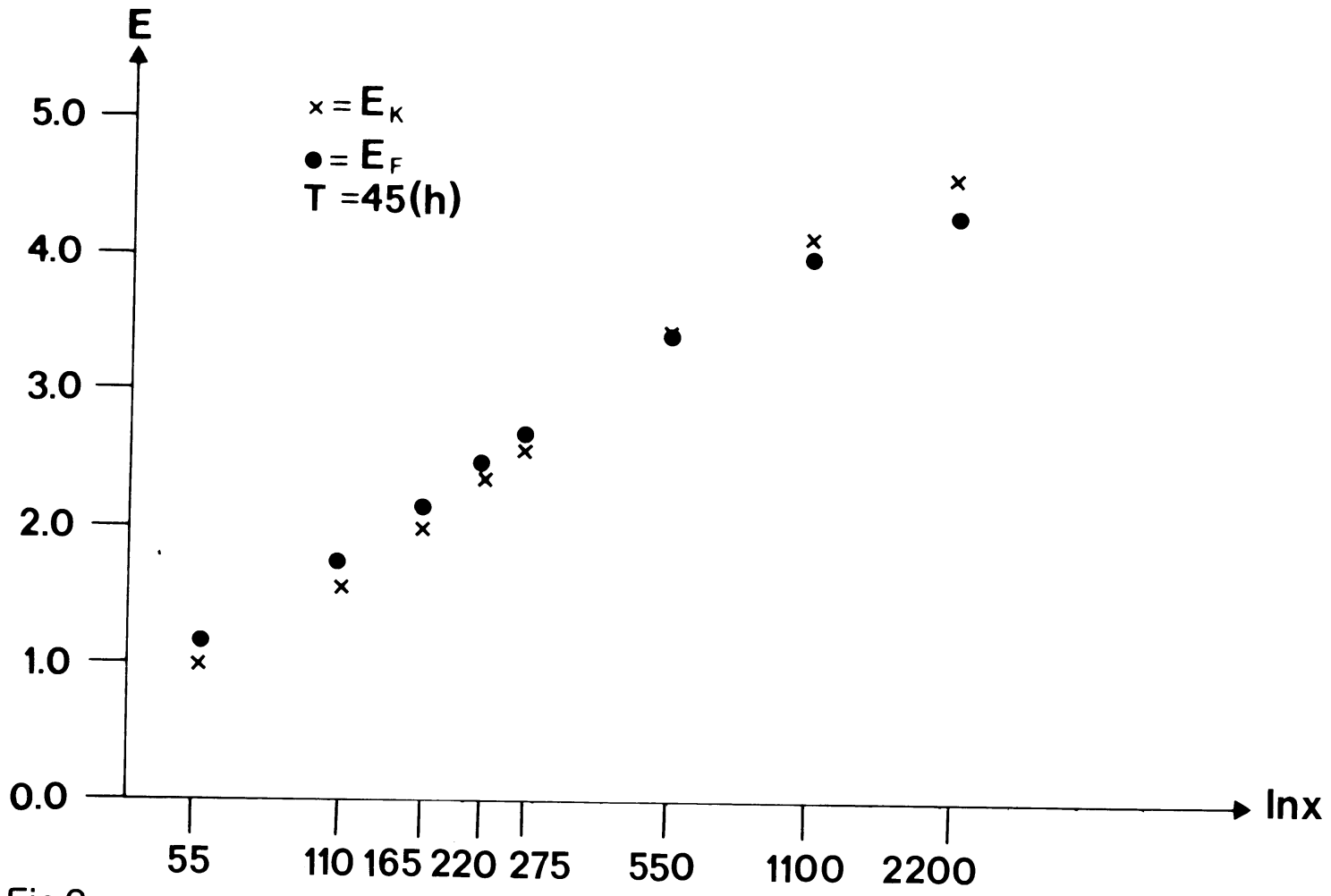

Fig 6

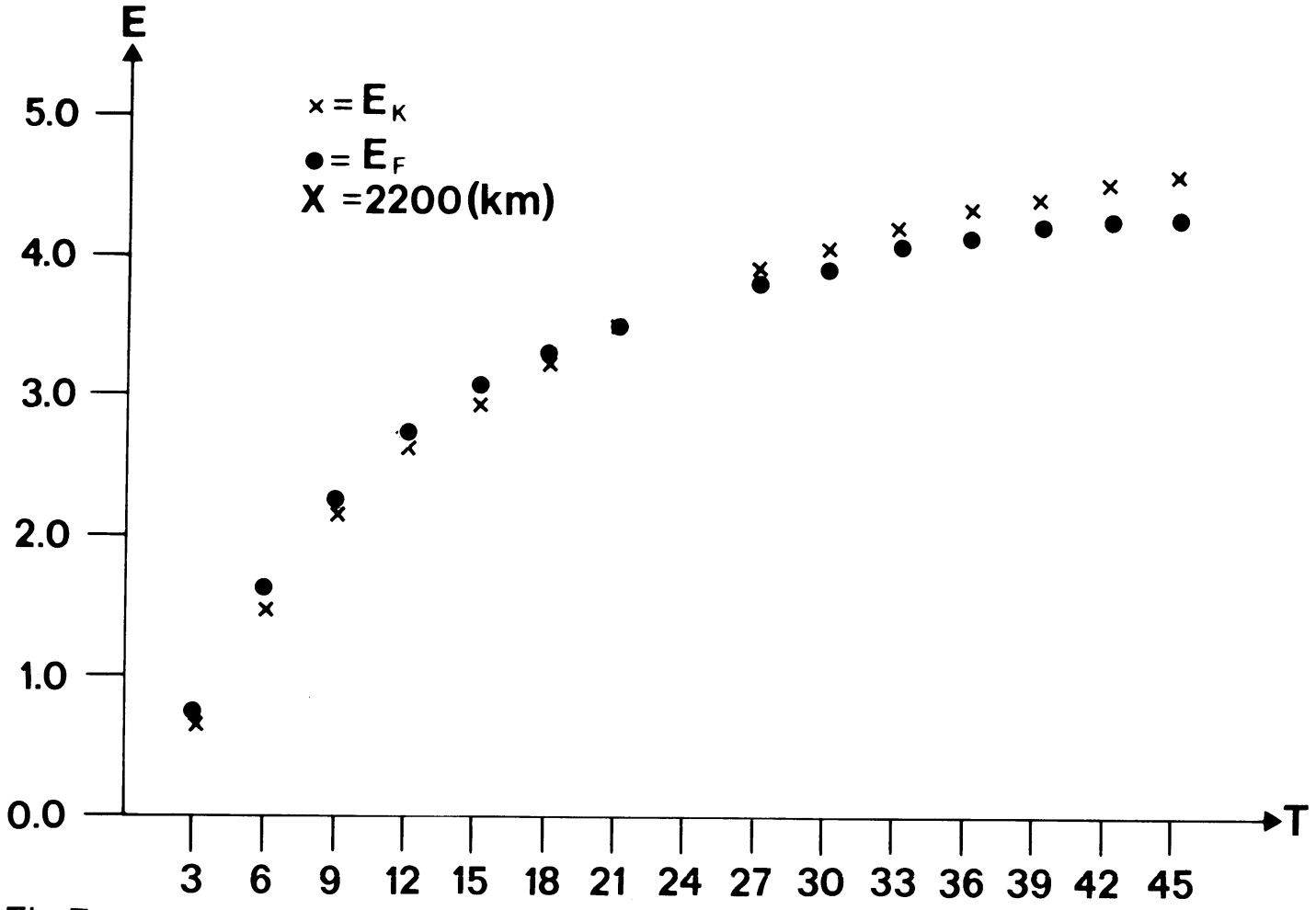
E
5.0
4.0
3.0
2.0
1.0
0.0
× = E_K
● = E_F
X =2200(km)
T
3
6
9
12
15
18
21
24
27
30
33
36
39
42
45

Fig 7

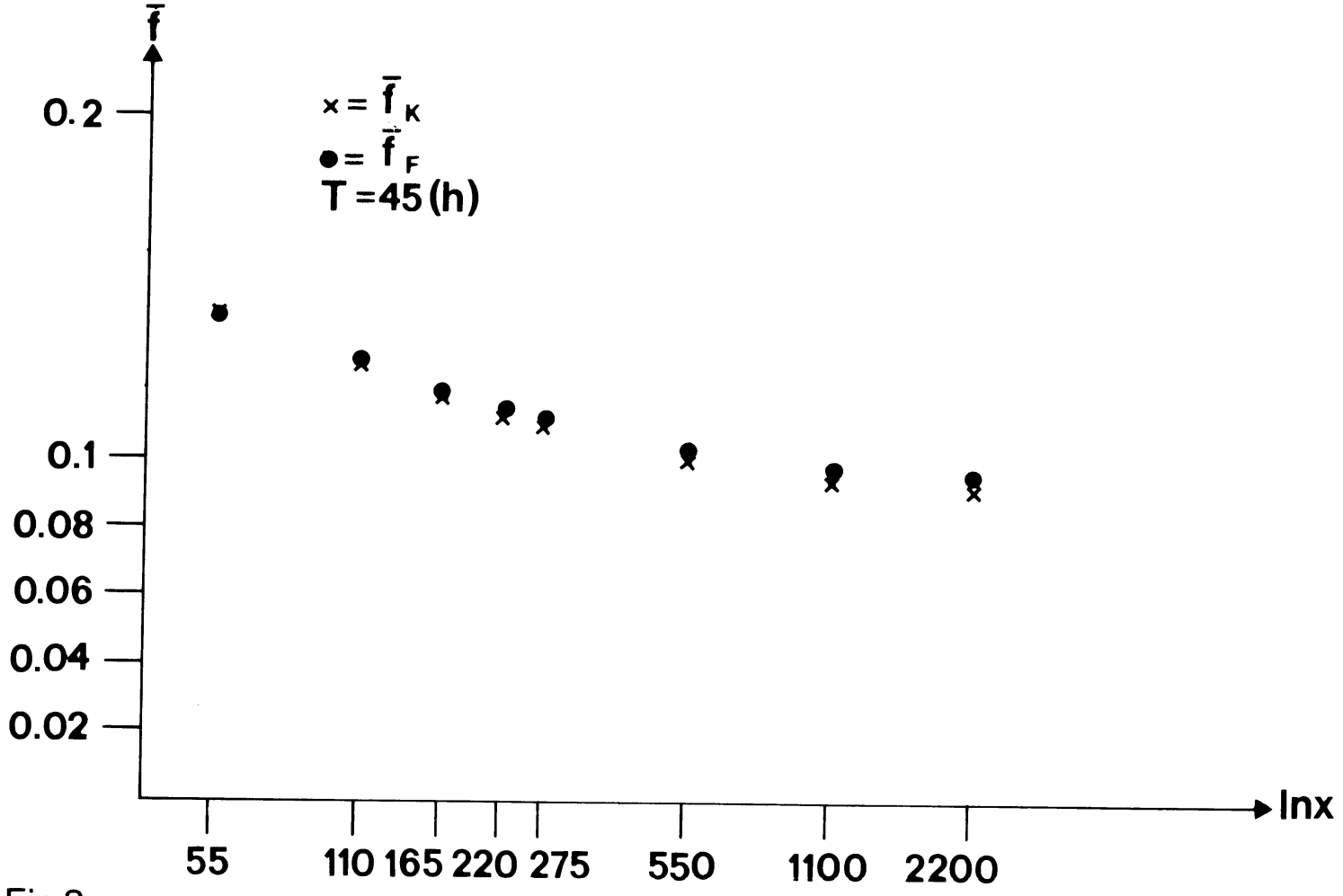
$\bar{f}$
0.2
0.1
0.08
0.06
0.04
0.02
× = $\bar{f}_K$
● = $\bar{f}_F$
T = 45 (h)
lnx
55
110
165
220
275
550
1100
2200

Fig 8

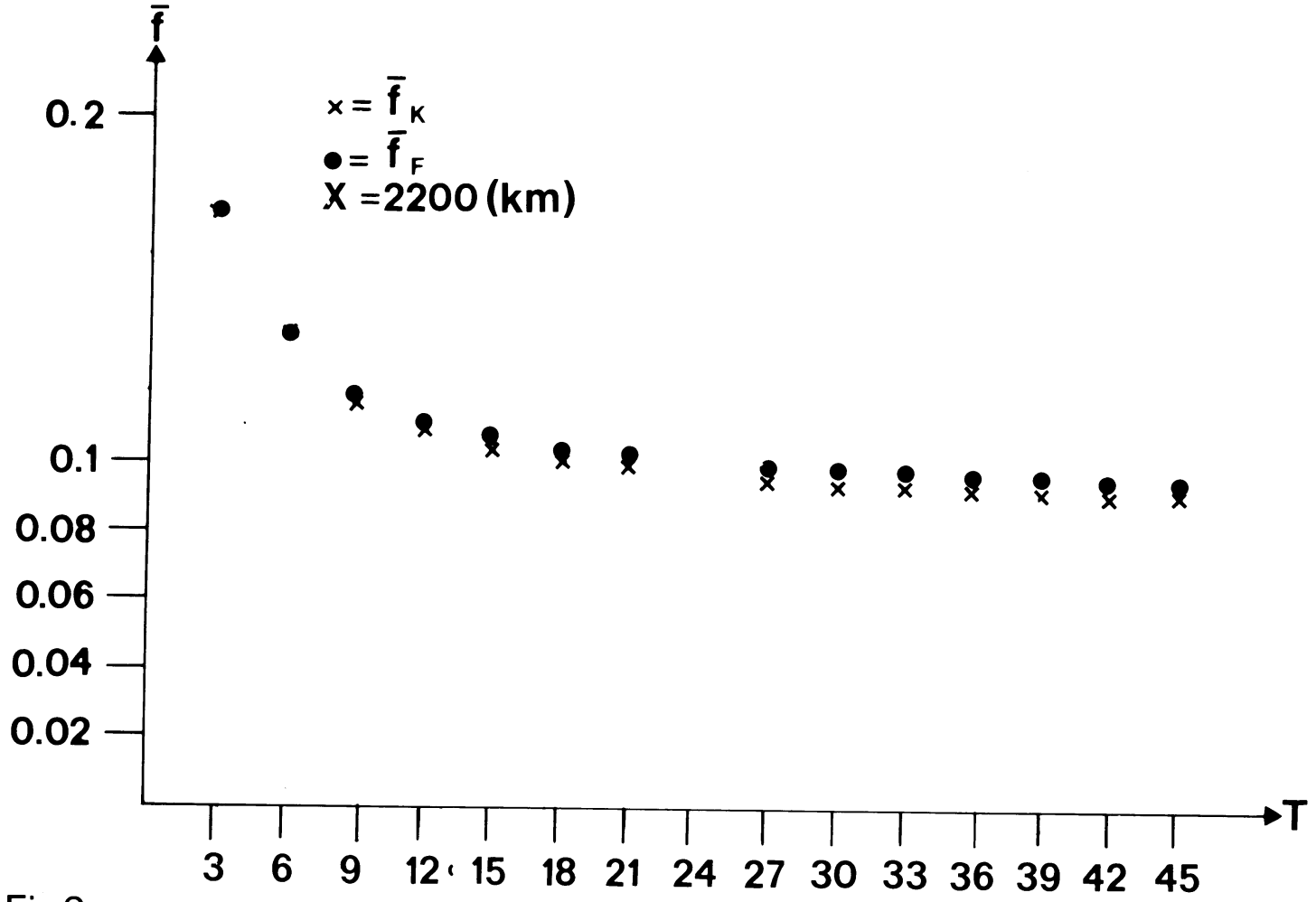
$\bar{f}$
0.2
0.1
0.08
0.06
0.04
0.02
× = $\bar{f}_K$
● = $\bar{f}_F$
X =2200 (km)
T
3
6
9
12
15
18
21
24
27
30
33
36
39
42
45

Fig 9